HEAT AND MASS TRANSFER WITH DRYING OF WATER-BASED VARNISHES

J. MINTZLAFF AND F. MAYINGER
Lehrstuhl A für Thermodynamik
Technische Universität München
85747 Garching

Abstract. This study deals with the drying of a dispersed varnish which is applied as a thin film on paper. Global measurements are performed in order to record the drying curves, whereas single phenomena are examined by local measurements. Their results are shown, and the basic equations for the calculation of the drying are presented.

1. Introduction

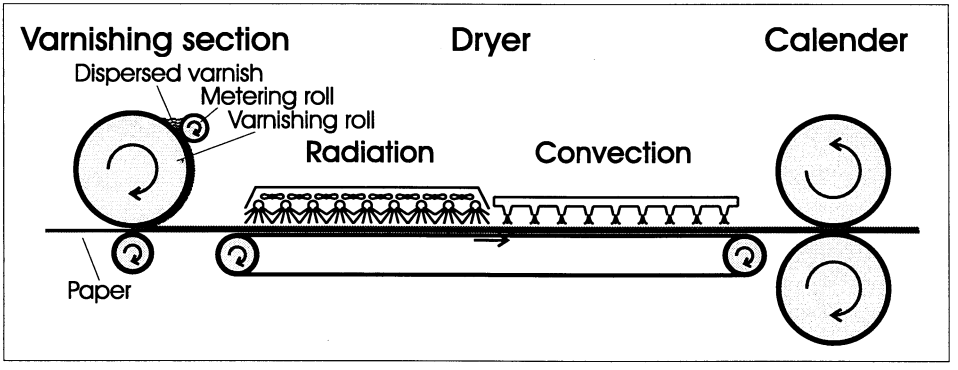

Figure 1. Varnishing machine

The objective of print finishing is the improvement of the optical, mechanical and physical properties of paper by applying a coating. Examples of such process products are high quality packings, money bills, or playing

cards. New laws concerning environmental protection have led to a change from solvent- to water- based varnishes within the last years. These lacquers consist of water and thermoplasts whose one half is dispersed and the other is solved in the water. Their drying behaviour is different from that of the former used varnishes, the solvent volatility is lower. The drying process requires much energy and thus contains a high potential for energy conservation.

Varnishing consists of three steps: Applying of the coating, drying and, if required, calendering as it is depicted in figure 1. This investigation focuses on the phenomena in the drying section of a varnishing machine which incorporates convective and radiative modules. These two drying methods, convection and radiation, are investigated in order to optimize the drying section and to provide an instrument for the design of a combined convective and radiative dryer. As a result the size, the energy consumption, and as a consequence the costs of the varnishing machines can be reduced.

2. Method of Investigation

In order to compare the different drying methods and to get an idea of their function, global measurements have been performed. The drying curves have been taken with different combinations of the following parameters: the temperature, the velocity and the humidity of the drying air, the spatial arrangement of the nozzles, the radiative power and wavelength and the thickness of the applied varnish.

The knowledge of the thermal and hydrodynamical boundary layer of the drying air flow over the varnished paper as well as of the processes within the drying coating is of major importance for the effective enhancement of the heat and mass transfer in the drying section. Therefore local investigations of the thermal boundary layer have been performed using the optical measurement technique of holographic interferometry in combination with balancing measurements. In order to obtain the required parameters for the numerical simulation of the drying process further local measurements have been carried out: micrographs of the coated paper, gravimetrical investigations of the desorption isotherms, examinations of the radiation field, and an analysis of the absorption spectrum of the drying material.

Finally the drying process is simulated numerically using the results of the local measurements. These calculations are verified by comparing their results to the global and industrial investigations. The simulation program is then implemented for the design of varnishing machines.

3. Global Investigations

3.1. EXPERIMENTAL SET-UP

For these measurements an experimental facility has been designed and set up as it is shown in figure 2. Process-air passes a conditioning unit where it adopts a defined humidity and temperature. It is then either blown into the radiative segment or through a heating element into the convective drying segment. Having passed the coated paper it is drawn off.

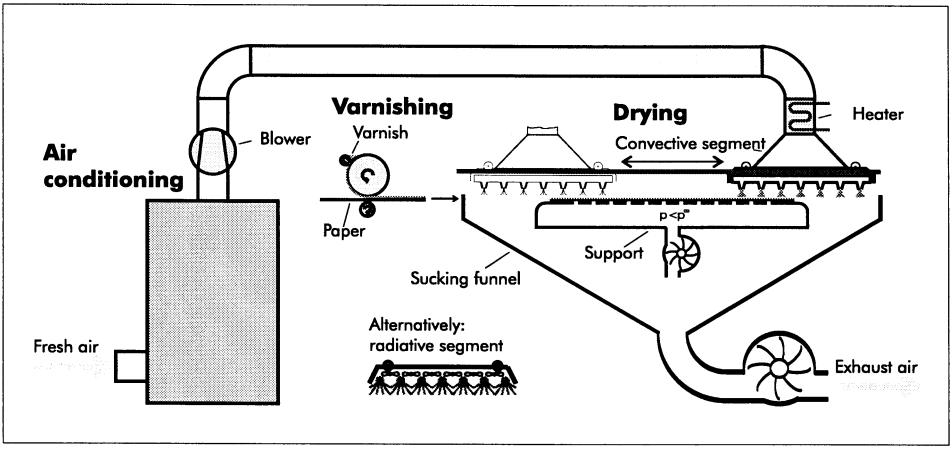

Figure 2. Experimental installation

The paper which has a size of 900 mm vs. 195 mm and a basis weight of 180 g/m^2 is coated in the varnishing unit while the drying segment is on the opposite side of the unit. As soon as the coated paper is placed on the support the drying segment starts moving back and forth above the paper in order to simulate a continuos movement of the paper in the industrial varnishing machine.

The moisture of the coated paper has been determined by means of a photometer by IR-reflection, the surface temperature has been measured with a pyrometer.

3.2. CONVECTIVE DRYING

The examinations have been performed by varying the temperature, the velocity, and the humidity of the drying air, and the spatial arrangement of the nozzles as it is illustrated in figure 3. The distance between the nozzles and the paper was 31 mm.

In terms of the drying behaviour it has been proved that the drying of the homogenious varnish, as it can be seen later, shows the same behaviour as it is known of porous bodies (figure 4). A starting period is followed by a constant rate period and a falling rate period afterwards.

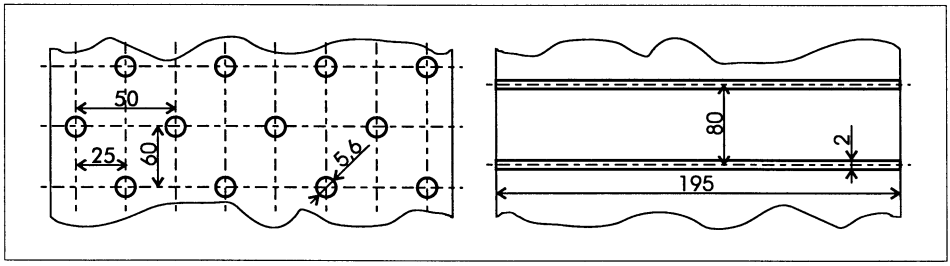

Figure 3. Nozzle arrangment of the convective drying segment

When using high temperatures or airflows a higher drying rate is achieved. This fact leads to a prolongation of the starting period. This might cause the onset of the falling rate period before the steady state conditions of the constant rate period are established which can be seen in figure 5. By drying with a significant drying rate only the equilibrium moisture which the pure paper had before varnishing can be achieved. This is the level 12.5 g/m^2 in the diagram.

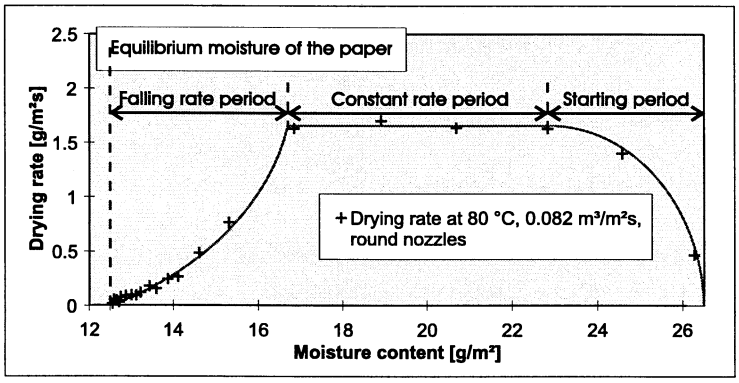

Figure 4. Drying behaviour of the water borne coating

Comparing the different spatial arrangements at equal temperatures and equal air flows, the round nozzles show better results as it is depicted in figure 5. As expected, this effect can only be observed in the constant

rate period with the mass transfer resistance lying in the hydrodynamical boundary layer. In the falling rate period the drying rates of both types of nozzles are identical.

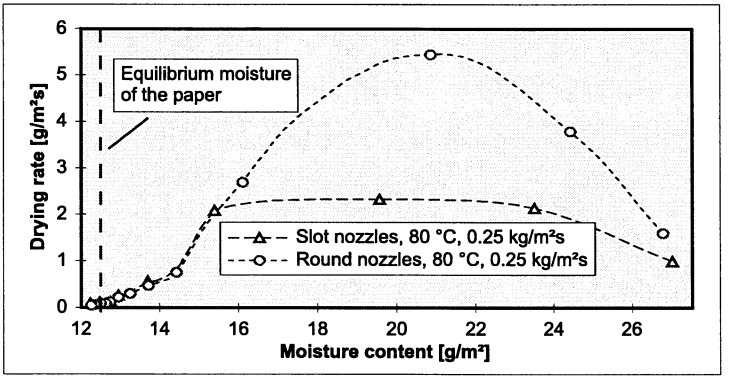

Figure 5. Drying curves of round and slot nozzles at 80 °C and 0.25 m^3/m^2s

3.3. RADIATIVE DRYING

The radiative segment is based on five quartz glass IR tubes with a distance of 100 mm to one another and with an angle of 60 ^{o} in direction of the longitudinal axis. They are located at a distance of 134 mm above the paper as it is illustrated in figure 6.

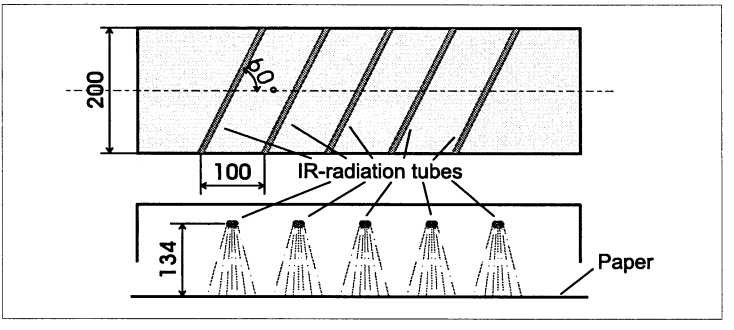

Figure 6. Drying segment for IR-radiation

The drying curves for short- and medium-wave IR-radiation with an electrical power of 25 kW/m^2 can be seen in figure 7. Wet varnish of an

amount of 26 g/m^2 has been applied. The striking difference from the convective drying is the fact that the coated paper can be dryed underneath the equilibrium level of the pure paper. It can be overdried. The maximum drying rate is lower than that with convection but at low moisture contents drying rate is higher with radiation.

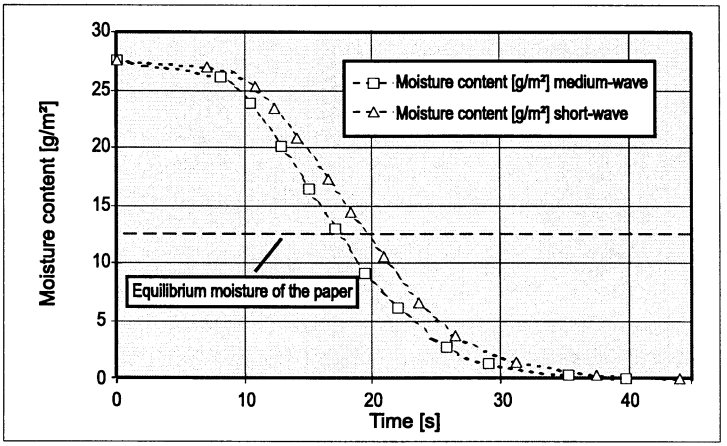

Figure 7. Drying curves for medium- and short-wave IR-radiation at 25 kW/m^2

A comparison with the two radiation curves shows that 12.5 % less time for the drying down to equilibrium moisture with medium-wave IR-radiation are required. This fact is caused by two phenomena (Siegel *et al.*, 1988). The absorption bands of water are stronger in the medium-wave spectrum. The short-wave radiation penetrates more deeply into the coated paper. The heat then has to be conducted to the surface of the lacquer while a portion of the heat gets lost from the bottom surface of the paper. The surface temperature is 80 ^oC when the equilibrium moisture is reached.

3.4. COMBINED CONVECTIVE AND RADIATIVE DRYING

In order to incorporate the advantages of both types of drying segments a combined segment has been set up as it is shown in figure 8. Drying air reaches a common space above the IR-tubes and is spread among the round nozzles which are in between the radiative tubes. The air becomes hot in the common space by the waste heat of the IR-tubes and in the nozzles which are affected by the radiation field. Therefore no additional heating element is required.

Figure 9 shows the drying curves of the combined drying segment with medium-wave tubes for two different air flows. The amount of $26g/m^2$ has

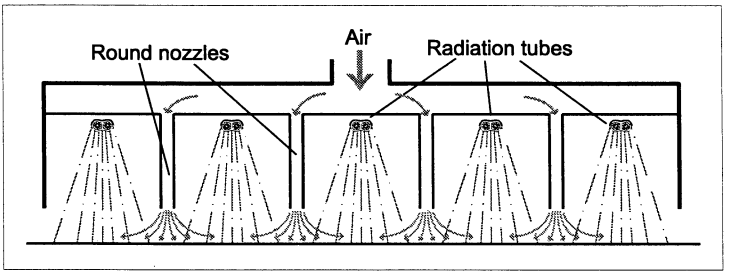

Figure 8. Combined drying segment for convection and IR-radiation

again been applied. The bigger air flow causes a shorter starting phase and a higher drying rate at high moistures. At lower moistures the drying rate increases with the lower air flow. Underneath the equilibrium moisture of the paper, drying with a lower air flow is even faster. Compared to pure radiative drying the time which is needed to achieve the equilibrium moisture is achieved is shorter by 20%. The surface temperature at equilibrium is $60°C$, $20K$ less than with pure radiation. This means that fewer cooling segments are required behind the drying section in the industrial process.

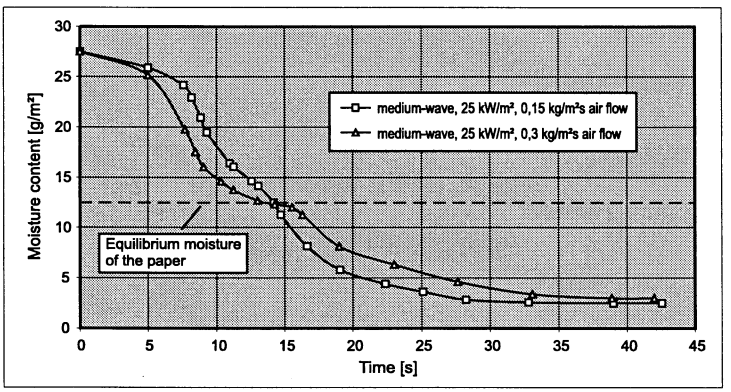

Figure 9. Drying curve of the combined drying segment

3.5. COMPARISON BETWEEN THE DIFFERENT DRYING SEGMENTS

The drying rates vs. the moisture content of the three drying segments are shown in figure 10. For all three drying methods the starting moisture was 15.0 g/m^2 above the equilibrium moisture of the pure paper which is 27.5 g/m^2 in total. The comparison shows that the maximum of the drying rate

of the combined segment which is caused by the convectional part is not as high as the maximum of the pure convectional drying. In the region of the lower moisture contents, however, the drying rate is nearly as high as that with pure radiation but with a surface temperature at the end of the drying that is $20K$ lower.

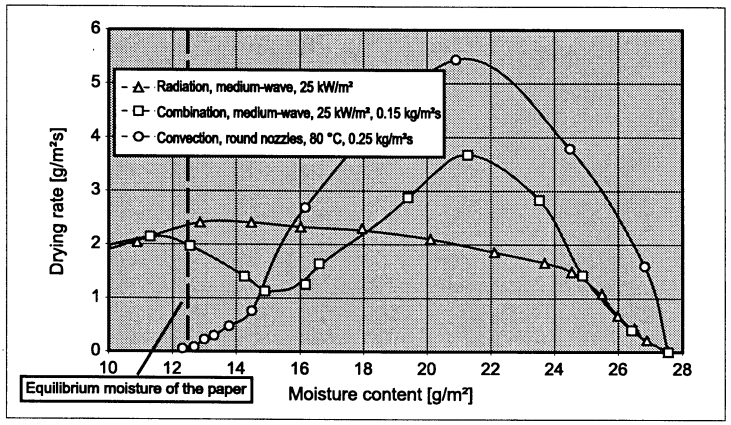

Figure 10. Drying curves for convective, radiative and combined drying

An optimized line-up for the dryer of an industrial varnishing machine starts with convective drying to utilize its high drying rates in the first drying section. Combined segments succeed in each of which the air flow is adapted to the moisture content.

4. Local Investigations

For a better understanding local investigations have been carried out to examine the single phenomena involved in the drying process.

4.1. COATING

For the later calculation of the drying it was of major importance to know the microscopical structure and the penetration behaviour of the varnish on the paper. Therefore scanning electron micrographs have been made of the cross section of the coated paper (figure 11) which have proved the varnish to be homogenious without any pores. The mass transfer of the water in the coating has to be calculated according to the laws of liquid diffusion (Reid *et al.*, 1987).

From several micrographs with different thicknesses of the film a connection with the penetrated ratio could be obtained (figure 12). It is proved

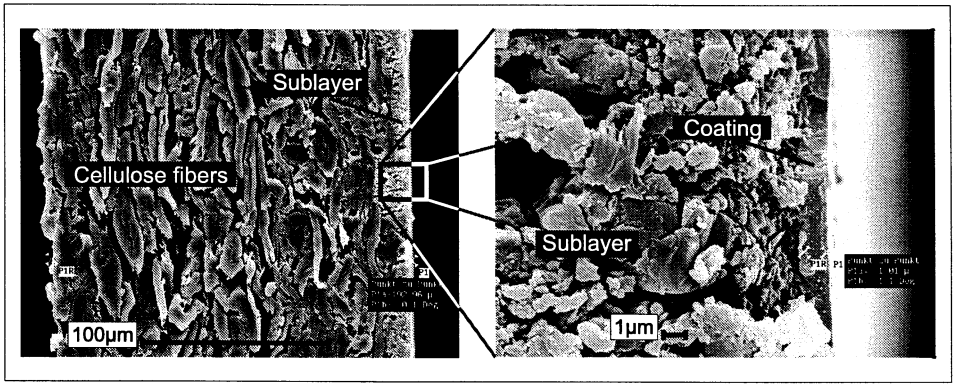

Figure 11. Scanning electron micrograph of the cross section of a coated paper

that within the examined range it can be assumed with a good precision that the ratio is constant.

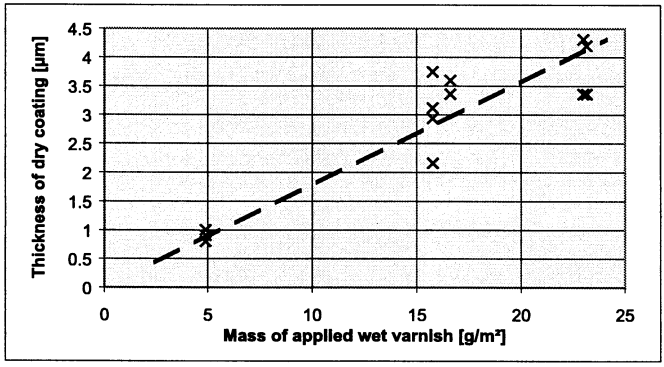

Figure 12. Thickness of dry film vs. applied wet mass

4.2. BOUNDARY LAYER OF THE DRYING AIR

Knowledge of the boundary layer of the drying air above the varnish is essential for the determination of the heat transfer coefficient. On the other hand with a given heat transfer coefficient it is possible to calculate the mass transfer coefficient according to the analogy of heat and mass transfer, since the *Lewis−number* equals 0.937 which is close to 1 (Baehr, Stephan, 1994).

By the means of the holographical interferometry it is possible to record a two dimensional temperature field (Mayinger *et al.*, 1994). Figure 13

shows the interferograms of the boundary layer of half of the space between two slot nozzles and two rows of round nozzles respectively at the same air flow. The dark lines can be regarded as isotherms.

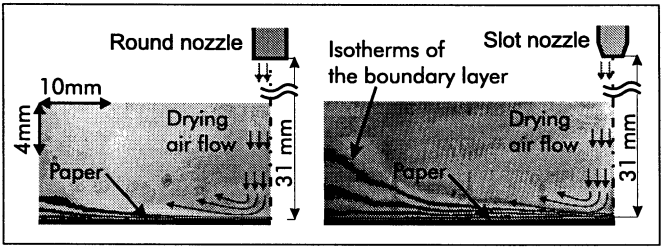

Figure 13. Interferograms for convection with round and slot nozzles

It can easily be seen that the considerably thinner boundary layer of the round nozzles causes a better heat and mass transfer. In bilancing examinations the heat transfer coefficients have been determined as shown in figure 14. These results correspond with the drying curves in figure 5.

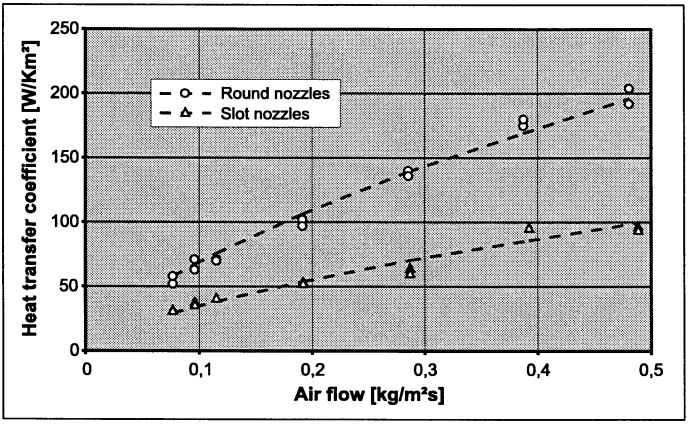

Figure 14. Value of the heat transfer coefficient vs. air flow for round and slot nozzles

The thinner boundary layer of the round nozzles is a result of the higher vertical speed of the air at the surface underneath the nozzles. In order to obtain equal velocities of the air jet at equal air flow rates the exiting nozzle area has to be of the same size. A nozzle width of 0.6 *mm* would have to be realized then. Regarding the costs of fabrication of the drying section of an industrial varnishing machine a width of 2 *mm* was chosen.

As a consequence, the starting velocity of the jet at the exit of the slot was about one third of the velocity of the round jet. An additional fact is that the boundary area relative to the cross-sectional area of the jet is bigger at the slot nozzle. Therefore the momentum exchange of this jet with the surrounding is bigger as well as its deceleration.

4.3. FURTHER LOCAL INVESTIGATIONS

Besides the shown examples further local investigations have been carried out such as measurements of the activity of the water in the varnish, examinations of the radiation underneath the drying segment or an analysis of the absorbing behaviour of IR-radiation of the coated paper. All these results are used for the numerical simulation which enables the calculation of the drying process.

5. Numerical Simulation - Basic Equations

After the experimental results the governing equations for the drying process are introduced especially to show what the results of the local measurements are required for.

5.1. ASSUMPTIONS

In order to enable the calculation of the drying some assumptions have been made to simplify the problem:

- Only transport processes rectangular to the surface are considered.
- The coated paper is divided into three zones: pure varnish, paper penetrated with varnish, pure paper.
- The mass transfer within the coating is merely caused by liquid diffusion because the lacquer does not have any pores.
- The bottom of the paper is adiabatic.
- The varnish is shrinking while drying.
- A system of coordinates based on the dry body is used which requires a transformation of coordinates. Water is then the only component which is moving within the grid .
- The convective energy term caused by diffusing water is negligible compared to the conducted energy.

5.2. MASS CONSERVATION

Since water is the only moving component in the system of coordinates based on the dry body the mass equation only has be set up for water (Saure, 1995).

$$\frac{\partial X}{\partial t} = \frac{\partial}{\partial \zeta}\left(\frac{D_{WL}}{(1+X\epsilon)^2}\frac{\partial X}{\partial \zeta}\right) \tag{1}$$

Here ϵ is the relation of the specific partial volumes.

$$\epsilon = \frac{\hat{V}_W}{\hat{V}_{L,dr}} \tag{2}$$

The transformed spatial coordinate is calculated by

$$\partial \zeta = \frac{\partial z}{1+X\epsilon} \tag{3}$$

The boundary conditions for $t > 0$ are at the bottom

$$\frac{\partial X}{\partial \zeta} = 0 \tag{4}$$

and at the top

$$\frac{\partial X}{\partial \zeta} = \frac{(1+X\epsilon)^2}{D_{WL}\rho_{L,dr}} \cdot \dot{m}_{W,ev} \tag{5}$$

The evaporated flux of water $\dot{m}_{W,ev}$ can be calculated as following (Mersmann, 1980):

$$\dot{m}_{W,ev} = \frac{\beta_h}{R_V T_m}(a_W p_{Vp} - p_{V,No}) \tag{6}$$

The activity a_W is taken from the local measurements and the mass transfer coefficient for the semipermeable boundary layer β_h can be calculated from the heat transfer coefficient α which also has been measured:

$$\beta_h = \frac{\alpha}{\bar{c}_{a,m}\bar{\rho}_{a,m}Le\left(1-\frac{p_{Vp}}{p}\right)} \tag{7}$$

According to the analogy of heat and mass transfer this calculation is possible since the air flow is turbulent and the Lewis-number $Le = 0.937$ is close to 1 (Baehr, Stephan, 1994).

5.3. ENERGY CONSERVATION

The energy equation is

$$\frac{\partial(\rho_{i,W}c_{i,W}) + \rho_{i,L}c_{i,L}) + \rho_{i,P}c_{i,P})}{\partial t} = \frac{\partial}{\partial z}\left(\lambda\frac{\partial T}{\partial z}\right) \tag{8}$$

The boundary conditions for $t > 0$ are at the bottom

$$\frac{\partial T}{\partial z} = 0 \tag{9}$$

and at the top

$$\frac{\partial T}{\partial z} = \alpha(T_{No} - T_{surface}) - \dot{m}_{W,ev}[r_o + c_{p,V}(T_\infty - T_{surface})] \tag{10}$$

This equation considers the convective heat transfer to the coated paper, the evaporation enthalpy of the evaporated water, and the energy flux caused by the vapour flux from the surface to the ambient air. The vapour reaches the temperature of the ambient air which leads to a reduction of the convective heat transfer (Kast *et al.*, 1992).

These equations are sufficient for a numerical simulation of the drying process. They provide an instrument for the future design of the optimized drying section of a varnishing machine.

6. Conclusions

Drying in general is quite a complex combined heat and mass transfer process. The difficulties arise from the complexity of the process and from the changing properties which are strongly affected by temperature and humidity. In case of the drying of a water-borne coating applied on paper it has been tried here to show the aspects for an entire treatment of this subject.

Global measurements provide the base of the investigation. They enabled the finding of the best nozzle arrangment for the convective and the optimum wave length for the radiative segment. With this knowledge a combined segment was created and tested. Regarding the requirements of each drying phase an optimized line up of the segments in the drying section of an industrial varnishing machine was found.

For the calculation of the drying process in local investigations the single phenomena involved in the drying process were examined. Furthermore the results proved to be in good correspondance with the global measurements.

Finally the basic equations for a calculation of the drying process have been introduced. They enable the numerical simulation and provide an instrument for the future design of the optimized drying section of a varnishing machine.

Nomenclature

a_W	activity of the water in the lacquer, -
c	specific heat, J/kg
$\bar{c}_{a,m}$	mean specific heat of the air in the boundary layer, J/kg
D_{WL}	Fickian diffusion coefficient of the water in the lacquer, m^2/s
Le	Lewis-number, -
$\dot{m}_{W,ev}$	evaporated flux of water, kg/m^2s
p_{Vp}	saturated state pressure of the vapour, Pa
$p_{V,No}$	partial pressure of vapour in the drying air, Pa
R_V	specific gas constant of vapour, $R_V = 462 J/kgK$
t	time, s
X	humidity referred to dry body, kg/kg
α	heat transfer coefficient, W/m^2K
β_h	mass transfer coefficient for the semipermeable boundary layer, m/s
ϵ	relation of the specific partial volumes, -
λ	thermal conductivity, W/Km
$\rho_{L,dr}$	density of the dried lacquer, kg/m^3
$\rho_{i,P}$	partial density of the paper, kg/m^3
$\rho_{i,W}$	partial density of the water, kg/m^3
$\bar{\rho}_{a,m}$	mean density of the air in the boundary layer, kg/m^3
ζ	transformed spatial coordinate, m

References

Baehr, H. D., Stephan, K. (1994) *Wärme und Stoffübertragung*. Springer-Verlag, Heidelberg

Kast, W., Krischer, O., Kröll, K. (1992) *Trocknungstechnik, Bd. 1 Die wissenschaftlichen Grundlagen der Trocknungstechnik*. Springer-Verlag, Heidelberg

Mayinger, F. (Ed.) (1994) *Optical Measurements*. Springer-Verlag, Heidelberg

Mersmann, A. (1980) *Thermische Verfahrenstechnik*. Springer-Verlag, Heidelberg

Reid, R. C., Prausnitz, J. M., Poling, B. E. (1987) *The Properties of Gases and Liquids*. McGraw-Hill Book Company, New York

Saure, R. (1995) *Zur Trocknung von lösemittelfeuchten Polymerfilmen*. VDI-Verlag, Düsseldorf

Siegel, R., Howell, R. H., Lohrengel, J. (1988) *Wärmeübertragung durch Strahlung, Teil 1 Grundlagen und Materialeigenschaften*. Springer-Verlag, Heidelberg